Biointerface Research in Applied Chemistry
Open-Access Journal (ISSN: 2069-5837)

Article
Volume 13, Issue 4, 2023, 396
https://doi.org/10.33263/BRIAC134.396

Investigation on Controlling Therapy of Bone Skeletal and Marrow Cancer: A Biophysical Chemistry and Molecular Dynamic Study of Bisphosphonates Interaction with Bone Structures

Fatemeh Mollaamin [1], Majid Monajjemi [2,*], Mitra Naeimi [3], Karim Zare [2]

[1] Department of Biomedical Engineering, Faculty of Engineering and Architecture, Kastamonu University, Kastamonu, Turkey; smollaamin@gmail.com (F.M.);
[2] Department of Chemical engineering, Central Tehran Branch, Islamic Azad University, Tehran, Iran; m_monajjemi@srbiau.ac.ir (M.M.);
[3] Department of Biomedical Engineering, Central Tehran Branch, Islamic Azad University, Tehran, Iran; mit.naeimi@iauctb.ac.ir (K.Z.);
* Correspondence: m_monajjemi@srbiau.ac.ir;

Scopus Author ID 6701810683
Received: 6.06.2022; Accepted: 4.08.2022; Published: 1.11.2022

Abstract: For more than four decades, the bisphosphonates family has been applied for osteoporosis and skeletal metastasis therapy. These drugs decrease the viability of cancer cells that are guided through the HER group of receptor tyrosine kinases. We discussed that bisphosphonates straightly bind to and inhibit HER kinases. In this study for docking a nitrogen-containing bisphosphonate with human FPPS and a few other targets, the iGEMDOCK docking software has been used. Nitrogen-containing bisphosphonates (NBPs) are mostly applied for bone treatment and also for the loss of skeletal disorders. The adsorption, retention, diffusion, and release of (NBPs) in bone are controlled by their affinities to such mineral compounds. Bisphosphonates have a high affinity for Ca^{2+} and therefore attack bone minerals, where they are internalized by bone-resorbing osteoclasts and inhibit osteoclast function. Nitrogen-containing bisphosphonates (NBPs), including Alendronate, Zolendronate, Risedronic, Ibandronate, and Pamidronate, are functionalized as effective inhibitors of bone resorption diseases. It targets FPPS (osteoclast farnesyl pyrophosphate synthase) to inhibit protein prenylation. Generally, the strong interaction sequence is as follows Alendronate > Risedronic > Pamidronate > Zolendronate > Ibandronate, and this was because of strong electrostatic interactions between amine groups and phosphate ions.

Keywords: iGEMDOCK docking; alendronate; risedronic; pamidronate; zolendronate; ibandronate; FPPS; bone cancer.

1. Introduction

1.1. Osteoclasts, osteoblasts, and osteocyte cells.

In contrast to the simple shape, bone is a complex and dynamic tissue that is rebuilt time by time. The restructured mechanism consists of two steps: 1- fresh bone is produced; 2- old bone is destroyed. The human has approximately 220 bones, including several different tissues: bone, cartilage, connective tissues, various blood tissues, adipose tissue, and nervous tissue. The bone matrix is a combination of 25% water, 25% collagen fibers, and 50%

crystallized mineral salts. Minerals salts are the reason bone hardens due to calcification by osteoblasts for the bone-building cells [1-5]. There are three major types of cells in the bone microenvironment: osteoclasts, osteoblasts, and osteocytes (Scheme1).

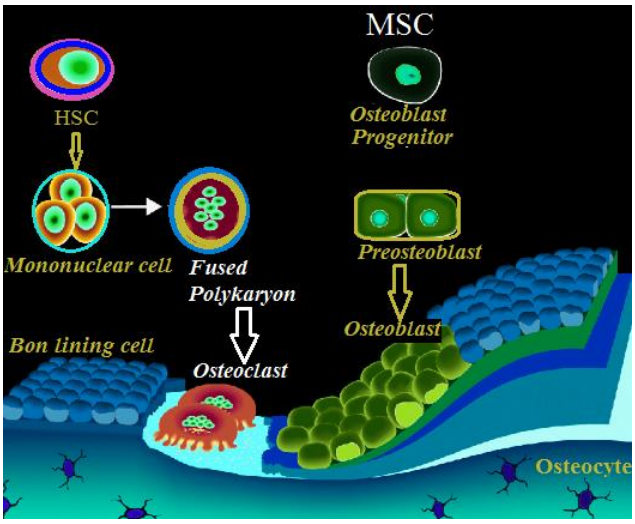

Scheme 1. Osteoclasts, osteoblasts, and osteocytes cells illustration.

Osteoclasts are huge cells extracted from a kind of white blood cell that releases a special acidic enzyme that digests the mineral components of the bone matrix. This breakdown of bone matrix, termed resorption, is the usual envelopment, growth, maintenance, and repair of the bone. Osteoblasts are the bone-building cells where that synthesize collagen fibers and other organic components needed for building the matrix of bone tissue and are finally converted to become osteocytes. Osteocytes are mature bone cells responsible for maintaining daily metabolism and exchanging nutrients and waste products with the blood [5-8]. Although bone hardness depends on the crystallized inorganic mineral salts, bone flexibility depends on collagen fibers that provide tensile strength and resistance to being stretched or torn apart. It is a notable lack of calcium during deregulated thick bumps tissues, making the bones overly flexible or vulnerable to fracture [1-3] and consequently, the tumor appears, which needs to develop the capability of creating new blood vessels for getting nutrients and oxygenation during angiogenesis process [8-12]. The bone microenvironment supports the establishment and orchestrates the expansion of malignant tumors in the bone. In this work, we are looking to control the balance between osteoclasts and osteoblasts because cancer therapy to repress growth has several toxic effects that affect the patient. Bone metastases are the root cause of cancer-related pain and can result in pathological fractures and paralysis. Now days compared with other types of cancers, the incidence of bone metastasis has increased extremely. Bone metastases have generally been divided into osteolytic or osteoblastic. Increased osteoclast activity causes cause osteolytic lesions in net bone resorption. On the other hand, osteoblastic lesions are formed via abnormal bone around tumor cell foci. Therefore, both types of metastasis appear by accelerated bone resorption, and related tumors-induced changes in bone metabolism can be monitored via the measurement of bone turnover markers. Obviously, under this condition, metastatic bone lesions, including osteolytic and osteoblastic of the normal bone remodeling process, become dysfunctional. For instance, breast cancer causes osteolytic metastases, while prostate cancer presents mostly with osteoblastic lesions. Collagen was radio graphically lytic; blastic indicates that all types of bone metastases contain an element of osteoclast activation, which has been confirmed histologically. The role of osteoclasts in metastatic bone lesions is that anti-resorption therapy reduces skeletal-related lytic or blastic

metastatic bone disease. Therefore, it cannot be recognized to understand the bone microenvironment and its manipulation by cancer. The idiom of the bone microenvironment interprets the complex bio-fundamental system that consists of hematopoietic and mesenchyme cells from multiple lineages with the sinusoidal blood made by bone marrow stromal. In marrow metastases, bone serves as the main source of growth factors or is used for the marrow cavity function for the coherence of the bone-tumors interactions. These cells, including osteoclasts, osteoblasts, and osteocytes, as well as several other same as myeloid, marrow, and hematopoietic cells, all interact with the metastatic process to different degrees. Over the past three decades, it has been confirmed that the bone is hugely rich in growth factors, including BMPs, IGFs, TGFb, FGFs, and PDGFs, with several kinds of metastases by releasing cytokines appear tumors cells [13]. Bone components, time by time, are modeled by the actions between various bone cells [14]. Consequently, the skeleton restructures to achieve its size by synthesis of bone at other points [15]. As soon as the bone shape appears at mature size, the process named remodeling commences, resulting in the continuous replacement of 'old' bone by newly formed tissue [14-16]. Bone restructuring usually appears at millimeter-scales along the skeleton, controlled by osteoblasts, osteoclasts, and basic multicellular units (BMU) [14]. Osteoclasts have differences with macrophage/monocyte and potentially result in bone resorption, either on the bone layers or via tunneling into the bone marrow [16]. By the end step of bone restructuring, osteoblasts, through calcium complexes, become mineralized [17], and osteocytes extracted from osteoblasts [18] are placed on the newly formed bone matrix. Bone structure stops in its situation until the next remodeling cycle begins [17]. During mature age and adult duration, formal bone restructuring is the main process toward healthy bone configuration and function. Youth adult cells restructure more than ten million bone units through the skeleton at any time. Notably, resorbing old bone and replacing it with an equal amount of new bone are equal to the total amount of bone mass. During aging, bone restructuring becomes increasingly imbalanced, and bone resorption occurs [16,17]. The bone restructuring phenomenon obeys osteoblasts that control the input signaling pules via the RANKL/RANK/OPG [19] by hormones and growth factors of cytokines. Osteoclast manufacturing occurs via a series of processing, consisting of proliferation, fusion, and activation [18,19]. The activation receptor ligand (RANKL) belongs to the TNF group that is translated through various genomes containing osteoblast lineage and T-cells and has been functionalized as a sensor signal in the regulation of osteoclast genesis or resorption (Scheme 2) [20–23].

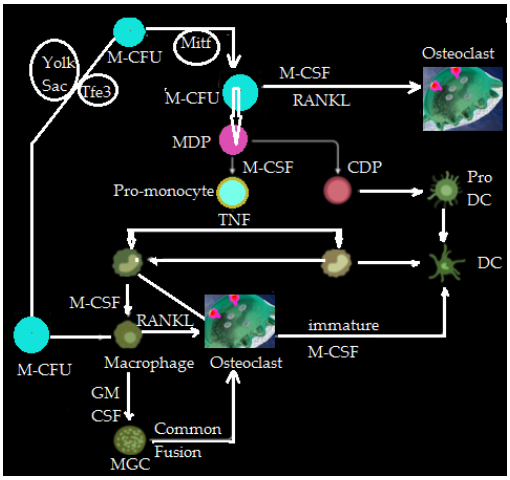

Scheme 2. The role function of Receptor activator of NF Kappa or RANKL with TNF, M-CSF, CDP, and M-CFU component in osteoprotegerin / osteoclastogenesis-inhibitory phenomenon.

RANKL causes osteoclast activation, and though those mice deficient in either RANK or RANKL are phenotypically equal, there are differences between osteoporosis and osteoclasts. These phenotypes completely exhibit the essential role of this receptor-ligand pair in bone configuration and restructuring [24,25]. The RANK–RANKL system is usually regulated via osteoprotegerin (OPG) that acts as a decoy receptor to RANKL, preventing RANKL from binding to RANK. OPG, translated as a secreted soluble protein, can block osteoclast and their activation, and its main role is counter-regulator of bone metabolism [26]. Several osteotropic and cytokines hormones can influence the genome translation OPG and RANKL [27,28], such as parathyroid (PTH), interleukins, and tumors necrosis factor-a (TNF-a) that increase the osteoblastic translation of RANKL to the related OPG.

On the other hand, treatment with OPG has been done as inhibit bone resorption in humans [29,30]. Boucharaba [31] studied controlling metastatic tumor growth in cell bone and explained the mechanism of osteolytic bone metastases in breast cancer. In principal, the idea describes how tumor cells communicate with osteoblasts, leading to osteoclast activation and accelerated bone resorption. This problem not only makes the suitable position for cancer to grow but also causes the release of growth factors into the destroyed bone cells. These growth factors then produce further tumor growth, resulting in the signals by cancer (Fig. 1). Agents secreted from cancer cells have a critical function in bone metastasis. Therefore, it has been well distinguished that breast or prostate cancer is able to metastasize via the release of signaling molecules to bone restructuring by parathyroid hormone-related protein (PTHrP) as well as vascular endothelial growth factor (VEGF) [31-35]. Among these items, the PTHrP, which was discovered as the causal hormone in hypercalcemia of malignancy (HMM), shares a common receptor with parathyroid hormone (PTH) [36,37]. Tumors extracted from PTHrP can activate osteoclastogenesis via osteoblasts via stimulating osteoblasts and stromal cells to increase RANKL and suppress OPG expression [36-38]. Other agents that stimulated osteoclast formation and, subsequently, osteolytic activities can be listed as interleukins, TNF-a, M-CSF, and endothelial growth factor (VEGF) (Scheme 2) [39]. Increasing RANKL in osteoblasts leads to osteoclast activation and increased bone resorption for two reasons: it destroys existing bone, and the bone microenvironment is suitable for metastatic tumors in growth factors and cytokines. Among the factors, TGF-b is particularly important in increasing the production of PTHrP in breast cancer cells. Clinical approaches exhibit that blocking TGF-b signaling might have benefits in patients with bone metastases [40–43].

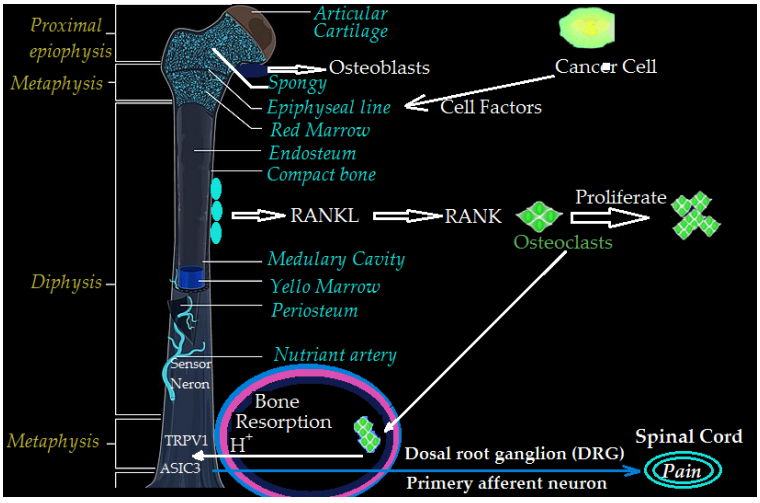

Figure 1. Mechanism of bone cancer pain.

Nowadays, two major categories of anti-resorptive treatments are used in medical clinks: bisphosphonates and the anti-RANKL antibody. Bisphosphonates have widely been applied to treat malignant hyperkalemia and skeletal metastasis in breast and prostate cancers [44].

1.2. Bisphosphonates.

Bisphosphonates belong to the family of the natural molecules pyrophosphate (P–O–P); the O atom in 'P–O–P' has been changed by a C atom, same as 'P–C–P' chemical bounds [45-47]. Bisphosphonates attach to bone minerals at sites of active bone resorption that keep up by resorbing osteoclasts. As soon as they insert into the cell, bisphosphonates' nitrogen atom inhibits farnesyl pyrophosphate synthase and prevents protein prenylation that interferes with normal cell metabolism and induces a profound decline in osteoclast-mediated bone resorption [46,48,49]. Some kinds of bisphosphonate molecules, such as ibandronate, have also exhibited anti-tumors properties *in vitro* [50,51]. Since separated bisphosphonate can be secreted from the bone skeleton in the resorption phenomenon, tumors might be exposed to a high density of BP *in vivo*. Such as alendronate that, in more than 120 mM concentrations, potentially produces transient high levels that affect cancer cells adjacent to osteoclasts [52]. Up to now, bisphosphonates such as Etidronate, Clodronate, Tiludronate, Alendronate, Residronate, Residronate, Ibandronate, Pamidronate, and Zoledronate have widely been applied by medical doctors as suitable effective way for the treatment of bone malignancies and stopping the secondary complications (Table 1) [53].

Etidronate is made up for treating a certain type of bone disease called Paget's that causes weakens osteoporosis and deforms bones. Clodronic acid or clodronate disodium is a non-nitrogenous bis-phosphonate that is also used as an anti-osteoporotic drug suitable for the prevention and treatment of osteoporosis in postmenopausal women and men to reduce vertebral fractures, hyperparathyroidism, hypercalcemia and myeloma for reducing related pains. Tiludronic acid or Tiludronate is a bisphosphonate applied to treat Paget's disease of bone, such as osteitis deforming. Its trade names are Tildren and Equidronate. It is approved for treating navicular disease and distal tarsal osteoarthritis in Europe [54]. Alendronic acid (Known as Fosamax) is a bisphosphonate used to treat osteoporosis and Paget's disease of bone and is taken by mouth with vitamin D and calcium compounds. General side effects appear with constipation, stomach pain, nausea, and acid reflux. This drug decreases the activity of cells that break down bone[55]. Risedronic acid with risedronate salt is a bisphosphonate that stops the activity of the fast-growing cells that break down bone and is used for the treatment or prevent osteoporosis, Paget's disease of bone and bone cancer. Ibandronic acid with Ibandronate salt has a bisphosphonate structure applied to prevent and treat osteoporosis and metastasis-associated skeletal fractures in people with cancer. It may also be used to treat hypercalcemia (elevated blood calcium levels). Pamidronic acid, pamidronate disodium, or APD, is a nitrogen-containing bisphosphonate used to prevent osteoporosis. Zoledronic acid, also known as zoledronate, is a medication applied to treat various bone problems, including osteoporosis, high blood calcium, bone breakdown, Paget's disease of bone, and Duchenne muscular dystrophy (DMD). Some side effects include fever, high blood pressure, diarrhea, and tiredness; more dangerous side effects include low blood calcium and osteonecrosis of the jaw. It works by blocking osteoclast cell activity and thus decreases bone breakdown [3].

1.3. Anti-RANKL treatments.

OPG as Anti-RANKL has potent anti-resorptive effects without direct cytotoxic actions. The binding of RANKL to its receptor RANK on the top of osteoclast cells is needed for osteoclast differentiation. With separating RANKL, OPG inhibits osteoclastogenesis and, thus, bone resorption both *in vitro* and *in vivo* [57,58]. In hospital treatment, OPG structure and anti-RANKL antibodies can be used to reduce bone resorption in patients with multiple myeloma or bone metastasis from breast cancer [59,60]. In addition, In prostate disease, treatment denosumab has been reported to delay the appearance of bone metastases [61].

1.4. Bisphosphonates therapy.

Bisphosphonates' majority of therapy extends towards removing osteoporosis and cancer metastasis in world countries. These kinds of drugs potentially kill cancer cells on osteoclasts. Absolute evidence indicates breast cancer patients treated with the potent bisphosphonate zoledronic acid reduce the size of cancer tumors [62,63]. Patients who use bisphosphonates for osteoporosis have a lower colon and breast cancer incidence. Up to now, the mechanism interpretation concerning this anticancer potential is not been well understood [64-66].

Table 1. Specific information on some bone disease drugs.

Bisphosphonates Compounds	Formula	Molar mass g/mol	Relative Potency	Code
Etidronate	$C_2H_8O_7P_2$	206.0282	1	CAS ID 7414-83-7
Clodronate	$CH_4Cl_2O_6P_2$	244.892	10	ChemSpider ID: 23731 ChEMBL Id: 12318 ATC code: M05BA02 (WHO)
Tiludronate	$C_7H_9ClO_6P_2S$	318.60	10	CAS Number 89987-06-4 ChEMBL Id: 1350 ATC code: M05BA05 (WHO)
Alendronate	$C_4H_{13}NO_7P_2$	249.096	100-500	CAS Number 66376-36-1 ChEMBL Id: 870 ATC code: M05BA04 (WHO)
Risedronate	$C_7H_{11}NO_7P_2$	283.112	1000	CAS Number 105462-24-6 ChEMBL Id: 923 ATC code: M05BA07 (WHO)
Ibandronate	$C_9H_{23}NO_7P_2$	319.231	500-1000	CAS Number 114084-78-5 ChEMBL Id: 997
Pamidronate	$C_3H_{11}NO_7P_2$	235.069	100	CAS Number 40391-99-9 ChEMBL Id: 834
Zoledronate	$C_5H_{10}N_2O_7P_2$	272.090	5000	CAS Number 118072-93-8 ChEMBL Id: 924 ATC code: M05BA08 (WHO)

N-containing bisphosphonates exhibit the most inhibiting farnesyl pyrophosphate synthase (FPPS) [65,67]. They can easily block cancer tumors because of T-cell receptor activation, NF inhibition, F, and hypoxia-inducible factor-1α suppression. Although there is no scientific ranking of antitumor or anti-FPPS properties among various bisphosphonates, suggesting that yet undiscovered phenomenon mediate their action on cancer cells [68-71]. About 35% of lung cancers are driven by activating mutations in the HER1 kinase domain, such as HER1E746-A750 and HER1L868R (18). Additionally, up to 95% of colon cancers

arise from the HER1 gene (22). Fortunately, bisphosphonates attach to the HER1/2, inhibit cancer signaling, and consequently kill bone, lung, breast, and colon cancer cells [72-74]. Although it is obvious that bisphosphonates inhibit FPPS's cancer potential to reduce bone resorption, there are several points of FPPS behavior that remain without any clear interpretation. Therefore drawing a map of connections among genes, diseases, and drugs might help us for resolving this unknown mechanism [72-78]. Yuen and coworkers [79] investigated osteoclasts from peripheral blood mononuclear cells extracted from three donors, exposed these cells to alendronate or risedronate, two of which are the most application of bisphosphonates, and performed microarrays on the isolated mRNA. The microarray dataset was used to develop a combined bisphosphonate gene signature by identifying genes that displayed statistical behavior across both alendronate- and risedronate-treated samples. This discovery was important because it exhibited that around half of the bisphosphonate-associated pathways contained HER family signaling molecules, including HER1, HER2/neu, EGF, phosphoinositide 3- kinase, and protein kinase B (AKT).

1.5. Aetiology and bone loss.

Women lose about 0.5% of their bone density during menopause per year. In addition, about 30% of women lose bone during the late period. Biochemical testing and medical analysis can distinguish women who are rapid losers, which means those who lose 4% to 6% of bone annually [80]. The dangerous problems for osteoporosis can be mentioned as; women more than men, age > 65, race, climate, early onset of menopause, longer periods, menopausal interval, and inactivity. Risk factors that may potentiate osteoporosis include: Smoking, alcohol abuse, excessive caffeine consumption, lack of dietary calcium and lack of sunlight exposure, and lack of vitamin D. The detect of osteoporosis is made in 3 ways: first; DXA method that bone mineral density measure through dual X-ray absorptiometry, second; biochemical testing and third bone biopsy with the pathological assessment that is certain method is radio graphical bone mineral density measurement (BMD). Several techniques are applied: single-photon absorptiometry, dual-photon absorptiometry, quantitative computed tomography, dual-energy x-ray absorptiometry, and ultrasonography for the most general section of bodies with the most risk for fracture: hip, wrist, and vertebrae. Evaluation of certain biochemical indexes of bone deformation, such as urinary N-telopeptide crosslinks, free pyridinoline, total deoxypyridinoline, hydroxyproline, serum osteocalcin, and also bone-specific ALP, are harmonized with longitudinal bone loss in old women (>60 years). These indexes might be helped same women who are at the most dangerous for bone loss [81, 82]. To evaluate bone deformation in women at menopause with vertebral osteoporosis, serum osteocalcin, urinary PYD, and DPD seem to be suitable indexes that have been applied so far [83,84].

2. Materials and Methods

2.1. Docking tools.

In this study for docking a nitrogen-containing bisphosphonate with human FPPS and a few other targets, the iGEMDOCK has been used. This software predicts how the small molecules bind to a target protein of known 3D structure, and the acceptable ligand can be distinguished as a suitable compound for the binding site in whole protein structures. This software can also help to define a suitable binding site based on the following steps of docking simulation: (a) definition of the binding site, (b) selecting the PDB files of the protein data

bank, (c) definition of the binding site type for new bounded ligand, (d) definition the center of the binding site by selected ligand, (e) definition the size of the binding site through the extended radius from the selected ligand. IGEMDOCK gives us an analysis with an image that can be visualized the docked states and categories through the protein-ligand interactions. So, the calculating steps can be saved in the output path, and each ligand's minimum energies will be distinguished for saving the data. The information on subsets might be considered a common trait. In addition, extracted data from the protein-ligand interactions and atomic composition can be accounted for by atomic types in different functional groups. Interaction aspects are extracted from the protein-ligand couples, and atomic combinations are calculated atomic types in various functional groups [85-89].

Advanced research algorithms, energy functions, and computational docking methods can add considerably to understanding the structural and energy basis of enzyme-substrate interactions.

Several ligands studied in this work contain Alendronate, Zolendronate, Risedronic, Ibandronate, and Pamidronate (Figure 2). The structure of these compounds is shown in Figure2 and Table 2. Various structures of human farnesyl pyrophosphate synthase were extracted from Protein Data Bank (PDB). In order to carry out the docking simulation, iGEMDOCK has been used as a molecular-docking package. It is suitable for accomplished docking of ligands binding to macromolecular receptors.

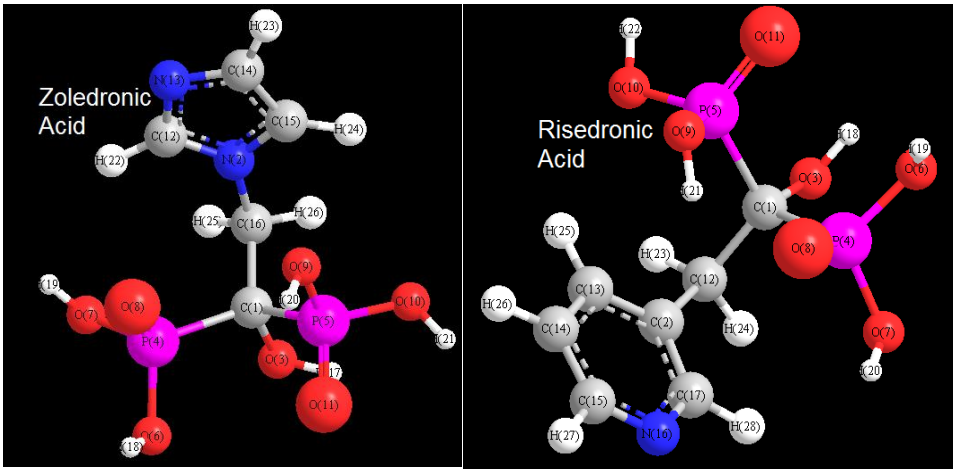

Figure 2. Optimization of Zolendronate, Risedronic with B3Lyp/cc-pvdz method.

Table 2. Atom type and atom name of Zolendronate, Risedronic for MD calculation.

Zoledronic Acid													
Name	**type**	**name**	**type**	**name**	**type**	**name**	**type**	**name**	**type**	**name**	**type**	**name**	**type**
C(1)	c3	P(5)	P5	O(9)	oh	N(13)	na	H(17)	ho	H(21)	ho	H(25)	h1
N(2)	na	O(6)	oh	O(10)	oh	C(14)	cc	H(18)	ho	H(22)	h5	H(26)	h1
O(3)	oh	O(7)	oh	O(11)	o	C(15)	cc	H(19)	ho	H(23)	h4	*H(27)	hn
P(4)	P5	O(8)	o	C(12)	cc	C(16)	c3	H(20)	ho	H(24)	h4		
Risedronic Acid													
C(1)	c3	P(5)	P5	O(9)	oh	C(13)	ca	C(17)	ca	H(21)	ho	H(25)	ha
C(2)	nb	O(6)	oh	O(10)	oh	C(14)	ca	H(18)	ho	H(22)	ho	H(26)	ha
O(3)	oh	O(7)	oh	O(11)	oh	C(15)	ca	H(19)	ho	H(23)	h1	H(27)	h4
P(4)	P5	O(8)	o	C(12)	c3	N(16)	c3	H(20)	ho	H(24)	h1	H(28)	

2.2. Preparation of ligand and target molecule.

By docking tool, the ligand and receptor were run, and the result of the simulation was analyzed. Besides starting, united atom charges, solvation parameters, and polar hydrogen were added into the receptor PDB file for protein preparation. The FPPS enzyme structure does not

have a ligand molecule, but it has water and phosphate molecule, which has been removed from its PDB file and make a free receptor. The rigid roots of each molecule were defined, and due to amide bonds being made non-rotatable, all rotatable dihedrals in the ligands were also assigned to allow them to rotate freely. Pre-calculated grid sheets are needed for any further Docking method for each ligand atom being docked, and it stores the potential energy arising from the interaction with the macromolecule. In docking situation of ligands in binding to protein is unknown because there is no pre-experimental information. One can only suppose that the minimum energy indicates the best ligand-protein complex. Information on docking for each ligand atom and potential energy arising from the interaction with related macromolecules has been saved. The grid box size was set at 50, 50, and 50 A° (x, y, and z), though it was changed depending on the ligand size.

The distance between grid points was fixed at around 0.4 A°. The Lamarckian Genetic Algorithm (LGA) was chosen to search for the best conformers. For each ligand, a maximum of 4 conformers was considered during docking. The size of the population was set to one hundred. The program LGA and pseudo-Solis and wets method were applied for minimization using default parameters [90-115] (Table 3, Figure 3).

Figure 3. Human FPPS complex with zoledronate by docking simulation.

Table 3. Docking parameter for all five ligands into protein farnesyl pyrophosphate synthase.

Docking Statistics					
Molecules	**Number of clusters**	**Cluster rank**	**Number of the cluster in conformation**	**Low binding energy (Kcal/mol)**	**Nunumber of run**
Risedronate	3	1 2 3	4 2 2	-7.65 -6.55 -7.25	6 4 2
Pamidronte	2	1 2	4 2	-6.50 -7.25	4 4
Zoledronate	3	1 2 3	2 4 2	-6.25 -6.75 -5.75	5 5 4
Alendronate	2	1 2	2 4	-7.75 -8.05	6 5
Ibandronate	3	1 2	2 4	-3.25 -3.75	4 3

3. Results and Discussion

3.1. Docking results.

Bisphosphonates have a high affinity for Ca^{2+} and therefore attack bone minerals, where they are internalized by bone-resorbing osteoclasts and inhibit osteoclast function. Nitrogen-

containing bisphosphonates (NBPs), including Alendronate, Zolendronate, Risedronic, Ibandronate, and Pamidronate, are functionalized as effective inhibitors of bone resorption diseases. It targets FPPS (osteoclast farnesyl pyrophosphate synthase) to inhibit protein prenylation, and it is a key branchpoint of the mevalonate pathway and catalyzes the successive condensation of isopentenyl pyrophosphate with dimethylallyl pyrophosphate and geranyl pyrophosphate [116,117]. In this study, the docking accuracy and scoring reliability for docking a nitrogen-containing bisphosphonate with human FPPS using docking software has been presented as the most potent drug for treating osteoporosis. FPPS (Figure 3) in mammals provides important lipid molecules, such as cholesterol and isoprenoids, which isoprenoids are needed for the prenylation of small GTPase signaling proteins for normal cellular activities [118,119]. The stopping of activity of this enzyme in this pathway is dangerous for various diseases, like inhibition of hydroxymethylglutaryl-CoA that reduces cholesterol biosynthesis, and inhibition of FPPS with the drug nitrogen-containing bisphosphonates (N-BPs) inhibit protein prenylation in osteoclast. Because of the special mechanism, N-BPs inhibit FPPS and prevent destroying of osteoclasts. Zoledronate (ZOL) is currently used to treat postmenopausal & steroid-induced osteoporosis. It is clear that FPPS is the major enzyme target of N-BPs, such as hypercalcemia, and osteolysis is associated with multiple myeloma and metastatic cancers [116-120]. Docking simulation of Alendronate, Zolendronate, Risedronic, Ibandronate, and Pamidronate linked to the active site of the FPPS make several conformers. The lowest binding energy of the docked complex was -8.05 kcal/mole for alendronate, and the highest energy was -3.25 for Ibandronate. In these complexes, the NH group of several amino acids of FPPS and the OH group of N-BPs acts as hydrogen bond donor. The bond distance between donors and acceptors atoms of hydrogen bonds varied between 1.8-2.05 Å with zoledronate, pamidronate, alendronate, and FPPS showed in Figure 4.

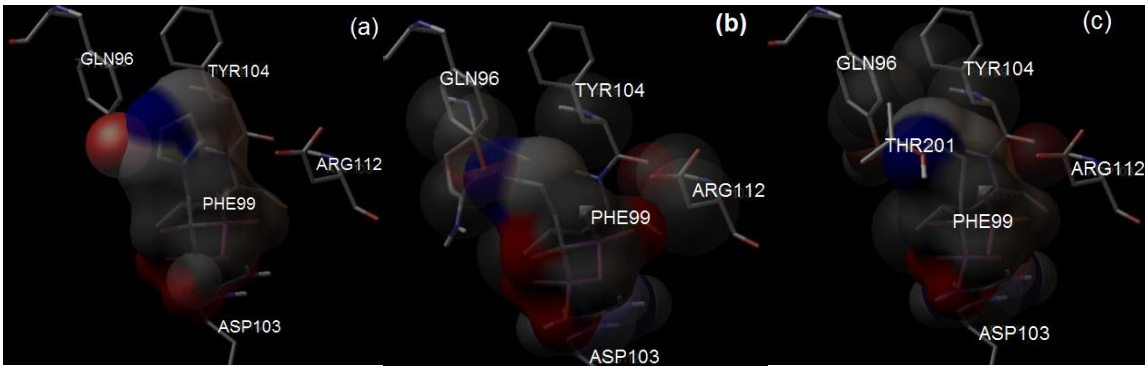

Figure 4. Docking of (**a**) Zoledronate; (**b**) pamidronate; (**c**) alendronate into FPPS.

Molecular docking simulation of Alendronate, Zolendronate, Risedronic, Ibandronate, and Pamidronate with receptor exhibits that the numbers of clusters with each ligand vary in several ranges of FPPS. Based on the minimum energy concept, it can be concluded that alendronate and risedronic acid is the two most suitable inhibitors for FPPS, amongst others considered in the study.

3.2. Molecular dynamic (MD) investigation.

The molecular structures of the NBPs were using B3Lyp/cc-pvdz level of method and basis sets. The optimized structures were used for atomic charge assignments through this method with the restrained electrostatic potential (RESP) method. The details of the atom types and atomic charges of the NBPs are presented in Tables4&5. The force fields such as amber,

charmm, and opls can only evaluate various conformational structures during MD simulations. Those force fields were parameterized using many protein-inhibitor complexes for which both structure and inhibition constants. The force fields evaluate binding in two steps; the first step, the intermolecular energy, should be calculated for the transition from those unbound states of the ligand and protein. The second step then calculates the intermolecular energy of binding the ligand and protein in suitable bound conformation. Theoretical Force fields are based on various interactions that are explained via spherically truncated Lennard–Jones potentials as follows: $V_{LJ}(r_{ij}) = 4\varepsilon_{ij}\{[\left(\frac{\sigma_{ij}}{r_{ij}}\right)^{12} - \left(\frac{\sigma_{ij}}{r_{ij}}\right)^{6}]\}, r < R_C$, $R_C$is a cutoff distance around 12 Å for VE. In addition, the Lorentz–Berthelot rules via arithmetic middle have been applied for the interactions among VE and h-BN atoms as follows "$\sigma_{ij} = 0.5(\sigma_i + \sigma_j)$"$and\ \varepsilon_{ij} = \sqrt{\varepsilon_i} * \sqrt{\varepsilon_j}$. The non-bonded and bonded parameters, including van der Waals of related force fields, are listed in Tables 4 and 5, for bisphosphonates. The total energy of the model system is a total of several partial energies as follows: E(system) = E(bond) + E(angle) + E(torsion) +E(over) +E(vdW) + E(Coulomb) + E(Specific), where E(bond) is the energy associated with the bond formation and (E(angle) + E(torsion)) are the energies associated with valence angle strain and torsional angle strain, respectively E(over) energies associated with valence angle strain and torsional angle strain, respectively, is an energy penalty term that prevents the over-coordination of the atoms. EvdW +E(Coulomb) is the dispersive, and electrostatic energy contribution between all atoms, respectively, and E(Specific) is a system-specific energy term that may include lone-pair, conjugation, and hydrogen binding (Table 4&5).

Table 4. Lennard–Jones potentials for MD simulation of Non-bonded parameters in terms of E (van der Waals) + E (Coulomb) $V_{LJ}(r_{ij}) = 4\varepsilon_{ij}\{[\left(\frac{\sigma_{ij}}{r_{ij}}\right)^{12} - \left(\frac{\sigma_{ij}}{r_{ij}}\right)^{6}]\}, r < R_C$.

Atom name	Atom type	Mass(g/mol)	$\sigma(nm)$	$\varepsilon(\frac{kcal}{mol})$
C(1)	c3	12.01	1.99	-0.101
N(2)	na	14.02	1.98	-0.093
O(3)	oh	16.03	1.95	-0.112
P(4)	P5	31.02	2.12	-0.061
P(5)	P5	31.02	2.13	-0.055
O(6)	oh	16.03	1.89	-0.084
O(7)	oh	16.03	1.92	-0.103
O(8)	o	16.03	1.99	-0.013
O(9)	oh	16.03	2.02	-0.018
O(10)	oh	16.03	2.04	-0.019
O(11)	o	16.03	2.00	-0.011
C(12)	cc	12.01	1.85	-0.019
N(13)	nc	14.02	1.96	-0.019
C(14)	cc	12.01	2.04	-0.011
C(15)	cc	12.01	1.92	-0.103
C(16)	c3	12.01	1.96	-0.029
H(17)	ho	1.01	1.32	-0.023
H(18)	ho	1.01	1.30	-0.021
H(19)	ho	1.01	1.34	-0.022
H(20)	ho	1.01	1.36	-0.019
H(21)	ho	1.01	1.28	-0.020
H(22)	h5	1.01	1.34	-0.021
H(23)	h4	1.01	1.38	-0.025
H(24)	h4	1.01	1.28	-0.022
H(25)	h1	1.01	1.32	-0.024
H(26)	h1	1.01	1.34	-0.022

The force field of charmm was developed by Karplus (Nobel prize [121]. The force field was not only parameterized for bulk properties but also interfacial thermodynamic

properties such as cleavage energy, solid-liquid interface energy, and immersion energy. Alendronate had larger binding free energies than the other and confirmed the docking result. Zolendronate was much more hydrophilic than the pyridine and bulky aliphatic groups of Risedronic and Ibandronate.

Computed binding free energies of Zolendronate to receptor matched the weak binding values in our measurements. Ibandronate showed the weakest binding free energies compared with the Risedronic in this work, which correlated with docking studies qualitatively. Generally, the strong interaction sequence is as follows Alendronate>Risedronic> Pamidronate>Zolendronate> Ibandronate, and this was because of strong electrostatic interactions between amine groups and phosphate ions [122-155].

Table 5. Parameters of bonded interactions of the atomistic force field.

Bonded & angle interaction

$$\{[V_b(r_{ij}) = \sum_{bonds} k_{ij}^b (r_{ij} - b_{ij})^2]\} + \{[V_\beta(\theta_{ijk}) = 0.5 \sum_{angle} k_{ijk}^\theta (\theta_{ijk} - \theta_{ijk}^0)^2]\} + \{[V(\varphi_{ijkl}) k_\varphi (1 + Cos(n\varphi - \delta)$$

bond	b(Å)	k^b kcal/mol*Å^2	angle	θ_{ijk}^0	k_{ijk}^θ $(\frac{kcal}{mol} * Rad^2)$	Dihedral	φ_{ijkl}	k_φ kcal/mol	n	δ
Zoledronic Acid										
R1 R(1,3),	1.42	220.5	A1 A(3,1,4),	108.2	50.8	D1 D(4,1,3,17)	-135.4	0.00	1	0.00
R2 R(1,4),	1.86	235.0	A2 A(3,1,5),	105.2	45.5	D2 D(5,1,3,17)	-19.8	0.05	1	0.00
R3 R(1,5),	1.86	240.5	A3 A(3,1,16),	106.6	60.5	D3 D(16,1,3,17)	101.4	0.00	1	0.00
R4 R(1,16),	1.53	300.0	A4 A(4,1,5),	108.2	53.0	D4 D(3,1,4,6)	43.5	0.05	1	0.00
R5 R(2,12),	1.26	320.5	A5 A(4,1,16),	114.0	46.9	D5 D(3,1,4,7)	-77.9	0.00	1	0.00
R6 R(2,15),	1.26	280.5	A6 A(5,1,16),	113.8	51.0	D6 D(3,1,4,8)	162.8	0.06	2	180.0
R7 R(2,16),	1.46	290.0	A7 A(12,2,15),	111.1	48.9	D7 D(5,1,4,6)	-70.1	0.08	1	0.00
R8 R(3,17),	0.96	420.0	A8 A(12,2,16),	124.7	46.5	D8 D(5,1,4,7)	168.3	0.55	1	0.00
R9 R(4,6),	1.60	385,0	A9 A(15,2,16),	124.1	39.5	D9 D(5,1,4,8)	49.2	0.05	1	0.00
R10 R(4,7),	1.60	275.0	A10 A(1,3,17),	109.3	35.8	D10 D(16,1,4,6)	162.0	0.09	2	0.00
R11 R(4,8),	1.49	246.0	A11 A(1,4,6),	110.5	40.5	D11 D(16,1,4,7)	40.5	0.60	3	0.00
R12 R(5,9),	1.60	300.0	A12 A(1,4,7),	110.0	41.6	D12 D(16,1,4,8)	-78.6	0.55	1	180.0
R13 R(5,10),	1.60	300.7	A13 A(1,4,8),	111.5	51.5	D13 D(3,1,5,9)	-179.2	0.45	1	0.00
R14 R(5,11),	1.49	240.0	A14 A(6,4,7),	109.4	48.0	D14 D(3,1,5,10)	57.8	0.44	1	0.00
R15 R(6,18),	0.94	220.5	A15 A(6,4,8),	107.3	46.0	D15 D(3,1,5,11)	-59.5	0.06	2	0.00
R16 R(7,19),	0.94	230.0	A16 A(7,4,8),	107.5	50.0	D16 D(4,1,5,9)	-63.6	0.00	3	180.0
R17 R(9,20),	0.94	240.5	A17 A(1,5,9),	111.3	49.0	D17 D(4,1,5,10)	173.4	0.00	1	0.00
R18 R(10,21),	0.94	220.5	A18 A(1,5,10),	109.4	47.5	D18 D(4,1,5,11)	56.0	0.33	1	0.00
R19 R(12,13),	1.26	230.0	A19 A(1,5,11),	110.2	51.0	D19 D(16,1,5,9)	64.2	0.23	1	180.0
R20 R(12,22),	1.09	240.5	A20 A(9,5,10),	111.9	45.8	D20 D(16,1,5,10)	-58.6	0.67	3	0.00
R21 R(13,14),	1.26	255.0	A21 A(9,5,11),	107.2	47.0	D21 D(16,1,5,11)	-176.0	0.00	2	0.00
R22 R(14,15),	1.34	238.0	A22 A(10,5,11),	106.5	44.0	D22 D(3,1,16,2)	-174.0	0.00	1	180.0
R23 R(14,23),	1.09									
R24 R(15,24),	1.09									
R25 R(16,25),	1.11									
R26 R(16,26),	1.11									

Bonded & angle interaction

$$\{[V_b(r_{ij}) = \sum_{bonds} k_{ij}^b (r_{ij} - b_{ij})^2]\} + \{[V_\beta(\theta_{ijk}) = 0.5 \sum_{angle} k_{ijk}^\theta (\theta_{ijk} - \theta_{ijk}^0)^2]\} + \{[V(\varphi_{ijkl})\, k_\varphi (1 + Cos(n\varphi - \delta)$$

bond	b(Å)	k^b kcal/mol*Å^2	angle	θ_{ijk}^0	k_{ijk}^θ $(\frac{\text{kcal}}{mol} * Rad^2)$	Dihedral	φ_{ijkl}	k_φ kcal/mol	n	δ
Zoledronic Acid										
			A23 A(4,6,18), 107.6 A24 A(4,7,19), 107.7 A25 A(5,9,20), 108.2 A26 A(5,10,21), 108.3			D23 D(3,1,16,25) 62.0 D24 D(3,1,16,26) -51.6 D25 D(4,1,16,2) 66.4 D26 D(4,1,16,25) -57.4				

4. Conclusions

This study examined how nitrogen-containing functional groups and surface protonation influenced the binding affinities of Alendronate, Zolendronate, Risedronic, Ibandronate, and Pamidronate through molecular simulation. Hydrophilic and hydrophobic behaviors of their nitrogen-containing functional groups differentiated their binding affinities to FPPS. Alendronate had larger binding free energies than the other and confirmed the docking result.

Funding

This research received no external funding.

Acknowledgments

The authors thank Kastamonu University and Islamic Azad University for providing computer and software equipment.

Conflicts of Interest

The authors declare no conflict of interest.

References

1. Han, G.; Wang, Y.; Bi, W.Z. Study on the health-related quality of life in patients after surgery for malignant bone tumors. *Asian Pac. J. Cancer Prev.* **2012**, *13*, 127–130, http://doi.org/10.7314/APJCP.2012.13.1.127.
2. Stokke, J.; Sung, L.; Gupta, A.; Lindber, A.; Rosenberg, A.R. Systematic review and meta-analysis of objective and subjective quality of life among pediatric, adolescent and young adult bone tumor survivors. *Pediatr. Blood Cancer* **2015**, *62*, 1616–1629, http://doi.org/10.1002/pbc.25514.
3. Frances, J.M.; Morris, C.D.; Arkader, A.; Nikolic, Z.G.; Healey, J.H. What is quality of life in children with bone sarcoma? *Clin. Orthop. Relat. Res.* **2007**, *459*, 34–39, http://doi.org/10.1097/BLO.0b013e31804f545d.
4. Tabone, M.D.; Rodary, C.; Oberlin, O.; Gentet, J.C.; Pacquement, H.; Kalifa, C. Quality of life of patients treated during childhood for a bone tumor: Assessment by the Child Health Questionnaire. *Pediatr. Blood Cancer* **2005**, *45*, 207–211, http://doi.org/10.1002/pbc.20297.
5. Ruggieri, P.; Mavrogenis, A.F.; Mercuri, M. Quality of life following limb-salvage surgery for bone sarcomas. *Expert Rev. Pharmacoecon Outcomes Res.* **2011**, *11*, 59–73, http://doi.org/10.1586/erp.10.91.
6. Aaronson, N.K.; Ahmedzai, S.; Bergman, B.; Bullinger, M.; Cull, A.; Duez, N.J.; Filiberti, A.; Flechtner, H.; Fleishman, S.B.; de Haes, J.C.; et al. The European Organization for Research and Treatment of Cancer QLQ-C30: A quality-of-life instrument for use in international clinical trials in oncology. *J. Natl. Cancer Inst.* **1993**, *85*, 365–376, http://doi.org/10.1093/jnci/85.5.365.

7. Bekkering, W.P.; Vlieland, T.P.; Koopman, H.M.; Schaap, G.R.; Schreuder, H.W.; Beishuizen, A.; Tissing, W.J.; Hoogerbrugge, P.M.; Anninga, J.K.; Taminiau, A.H. The Bt-DUX: Development of a subjective measure of health-related quality of life in patients who underwent surgery for lower extremity malignant bone tumor. *Pediatr. Blood Cancer* **2009**, *53*, 348–355, http://doi.org/10.1002/pbc.22078.
8. Bekkering, W.P.; Billing, L.; Grimer, R.J.; Vlieland, T.P.; Koopman, H.M.; Nelissen, R.G.; Taminiau, A.H. Translation and preliminary validation of the English version of the DUX questionnaire for lower extremity bone tumor patients (Bt-DUX): A disease-specific measure for quality of life. *J. Surg. Oncol.* **2013**, *107*, 353–359, http://doi.org/10.1002/jso.23218.
9. Liu, Y.; Hu, A.; Zhang, M.; Shi, C.; Zhang, X.; Zhang, J. Correlation between functional status and quality of life after surgery in patients with primary malignant bone tumor of the lower extremities. *Orthop. Nurs.* **2014**, *33*, 163–170, http://doi.org/10.1097/NOR.0000000000000050.
10. Bekkering, W.P.; Vliet Vlieland, T.P.; Koopman, H.M.; Schaap, G.R.; Beishuizen, A.; Anninga, J.K.; Wolterbeek, R.; Nelissen, R.G.; Taminiau, A.H. A prospective study on quality of life and functional outcome in children and adolescents after malignant bone tumor surgery. *Pediatr. Blood Cancer* **2012**, *58*, 978–985, http://doi.org/10.1002/pbc.23328.
11. Bekkering, W.P.; van Egmond-van Dam, J.C.; Bramer, J.A.M.; Beishuizen, A.; Fiocco, M.; Dijkstra, P.D.S. Quality of life after bone sarcoma surgery around the knee: A long-term follow-up study. *Eur. J. Cancer Care (Engl.)* **2017**, *26*, e12603, http://doi.org/10.1111/ecc.12603.
12. Kask, G.; Barner-Rasmussen, I.; Repo, J.P.; Kjäldman, M.; Kilk, K.; Blomqvist, C.; Tukiainen, E. Functional Outcome Measurement in Patients with Lower-Extremity Soft Tissue Sarcoma: A Systematic Literature Review. *Ann. Surg Oncol.* **2019**, *26*, 4707–4722, http://doi.org/10.1245/s10434-019-07698-w.
13. Hauschka, P.V.; Mavrakos, A.E.; Iafrati, M. D.; Doleman, S.E; Klagsbrun, M. Growth factors in bone matrix. Isolation of multiple types by affinity chromatography on heparin-Sepharose. *J Biol Chem* **1986**, *261*, 12665-74. https://doi.org/10.1016/S0021-9258(18)67143-1
14. Lemaire, V.; Tobin,F.L.; Greller, L.D.; Cho, C.R.; Suva, L.J. Modeling the interactions between osteoblast and osteoclast activities in bone remodeling. *J Theor Biol* **2004**, *229*, 293–309, http://doi.org/10.1016/j.jtbi.2004.03.023.
15. Frost, H.M.; Metabolism of bone. *N Engl J Med* **1973**, *289*, 864–5.
16. Parfitt, A.M. The mechanism of coupling: a role for the vasculature. Bone, **2000**, *26*, 319–323, http://doi.org/10.1016/S8756-3282(00)80937-0.
17. Aubin, J.E.; Advances in the osteoblast lineage. *Biochem Cell Biol* **1998**, *76*, 899–910. http://dx.doi.org/10.1139/bcb-76-6-899.
18. Aarden, E.M.; Burger, E.H.; Nijweide, P.J.; Function of osteocytes in bone. *J Cell Biochem* **1994**, *55*, 287–299, http://doi.org/10.1002/jcb.240550304.
19. Boyle, W.J.; Simonet, W.S.; Lacey, D.L. Osteoclast differentiation and activation. Nature, **2003**, *423*, 337–342, http://doi.org/10.1038/nature01658.
20. Anderson, D.M.; Maraskovsky, E.; Billingsley, W.L.; Dougall, W.C.; Tometsko, M.E.; Roux, E.R.; A homologue of the TNF receptor and its ligand enhance T-cell growth and dendritic-cell function. Nature **1997**, *390*, 175–179, http://doi.org/10.1038/36593.
21. Wong, B.R.; Rho, J.; Arron, J.; Robinson, E.; Orlinick, J.; Chao, M.; TRANCE is a novel ligand of the tumor necrosis factor receptor family that activates c-Jun N-terminal kinase in T cells. *J Biol Chem* **1997**, *272*, 25190–15194, http://doi.org/10.1074/jbc.272.40.25190.
22. Yasuda, H.; Shima, N.; Nakagawa, N.; Yamaguchi, K.; Kinosaki, M.; Mochizuki, S.; Osteoclast differentiation factor is a ligand for osteoprotegerin/ osteoclastogenesis-inhibitory factor and is identical to TRANCE/RANKL. *Proc Natl Acad Sci U S A.* **1998**, *95*, 3597–3602, http://doi.org/10.1073/pnas.95.7.3597.
23. Lacey, D.L.; Timms, E.; Tan, H.L.; Kelley, M.J.; Dunstan, C.R.; Burgess, T. Osteoprotegerin ligand is a cytokine that regulates osteoclast differentiation and activation. Cell. **1998**, *93*, 165–176, http://doi.org/10.1016/s0092-8674(00)81569-x
24. Kong , Y.Y.; Yoshida, H.; Sarosi, I.; Tan, H.L.; Timms, E.; Capparelli, C.; et al. OPGL is a key regulator of osteoclastogenesis, lymphocyte development and lymphnode organogenesis. *Nature* **1999**, *397*, 315–323, http://doi.org/10.1038/16852.
25. Li, J.; Sarosi, I.; Yan, X.Q.; Morony, S.; Capparelli, C.; Tan, H.L.; RANK is the intrinsic hematopoietic cell surface receptor that controls osteoclastogenesis and regulation of bone mass and calcium metabolism. *Proc Natl Acad Sci U S A.* **2000**, *97*, 1566–1571, http://doi.org/10.1073/pnas.97.4.1566.

26. Simonet ,W.S.; Lacey, D.L.; Dunstan, C.R.; Kelley, M.; Chang, M.S.; Luthy, R.; . Osteoprotegerin: a novel secreted protein involved in the regulation of bone density. *Cell.* **1997**, *89*, 309–319, http://doi.org/10.1016/s0092-8674(00)80209-3.
27. Hofbauer ,L.C.;Khosla, S.; Dunstan, C.R.; Lacey, D.L.; Boyle, W.J.; Riggs, B.L. The roles of osteoprotegerin and osteoprotegerin ligand in the paracrine regulation of bone resorption. *J Bone Miner Res* **2000**, *15*, 2–12, http://doi.org/10.1359/jbmr.2000.15.1.2.
28. Theill, L.E.; Boyle, W.J.; Penninger, J.M.; RANK-L and RANK: T cells, bone loss, and mammalian evolution. *Annu Rev Immunol.* **2002**, *20*, 795–823. http://doi.org/10.1146/annurev.immunol.20.100301.064753.
29. Bekker, P.J.; Holloway, D.; Nakanishi, A.; Arrighi, M.; Leese, P.T.; Dunstan, C.R. The effect of a single dose of osteoprotegerin in postmenopausal women. *J Bone Miner Res* **2001**, *16*, 348–360, http://doi.org/10.1359/jbmr.2001.16.2.348.
30. Bekker, P.J.; Holloway, D.L.; Rasmussen, A.S.; Murphy, R.; Martin, S.W.; Leese, P.T.; et al. A single-dose placebo-controlled study of AMG 162, a fully human monoclonal antibody to RANKL, in postmenopausal women. *J Bone Miner Res.* **2004**, *19*, 1059–1066, http://doi.org/10.1359/JBMR.040305.
31. Boucharaba, A.; Serre, C.M.; Gres, S.; Saulnier-Blache, J.S.; Bordet, J.C.; Guglielmi, J.; et al. Platelet-derived lysophosphatidic acid supports the progression of osteolytic bone metastases in breast cancer. *J Clin Invest.* **2004**, *114*, 1714–25, http://doi.org/10.1172/JCI22123.
32. Knupfer, H.; Preiss, R. Significance of interleukin-6 (IL-6) in breast cancer (review). Breast Cancer Research and Treatment **2007**, *102*, 129–135, http://doi.org/10.1007/s10549-006-9328-3.
33. Burtis, W.J.; Brady, T.G.; Orloff, J.J.; Ersbak, J.B.; Warrell, J.r , Olson, B.R, Immunochemical characterization of circulating parathyroid hormonerelated protein in patients with humoral hypercalcemia of cancer. *N Engl J Med.* **1990**, *322*, 1106–1112. http://doi.org/10.1056/NEJM199004193221603.
34. Kakonen , S.M.; Selander, K.S.; Chirgwin, J.M.; Yin, J.J.; Burns, S.; Rankin, W.A, et al. Transforming growth factor-beta stimulates parathyroid hormone-related protein and osteolytic metastases via Smad and mitogen-activated protein kinase signaling pathways. *J Biol Chem.* **2002**, *277*, 24571–24578, http://doi.org/10.1074/jbc.M202561200.
35. Li, J.; Karaplis, A.C.; Huang, D.C.; Siegel, P.M.; Camirand, A.; Yang, X.F, et al. PTHrP drives breast tumor initiation, progression, and metastasis in mice and is a potential therapy target. *J Clin Invest*. **2011**, *121*, 4655–4669, http://doi.org/10.1172/JCI46134.
36. Guise, T.A. Parathyroid hormone-related protein and bone metastases. *Cancer* **1997**, *80*, 1572–1580, http://doi.org/10.1002/(sici)1097-0142(19971015)80:8+<1572::aid-cncr7>3.3.co;2-d.
37. Capparelli, C.; Kostenuik, P.J.; Morony, S.; Starnes, C.; Weimann, B.; Van, G.; et al. osteoprotegerin prevents and reverses hypercalcemia in a murine model of humoral hypercalcemia of malignancy. *Cancer Res.***2000**, *60*,783–7.
38. Morony, S.;Warmington , K.; Adamu, S.; Asuncion, F.; Geng, Z.; Grisanti, M, et al. The inhibition of RANKL causes greater suppression of bone resorption and hypercalcemia compared with bisphosphonates in two models of humoral hypercalcemia of malignancy. *Endocrinology*, **2005**, *146*, 3235–3243, https://doi.org/10.1210/en.2004-1583.
39. Guise, T.A.; O'Keefe, R.; Randall, R.L.; Terek, R.M. Molecular biology and therapeutics in musculoskeletal oncology. *J Bone Joint Surg Am*. **2009**, *91*, 724–732, https://doi.org/10.2106/JBJS.I.00012.
40. Hu, Z.; Gupta, J.; Zhang, Z.; Gerseny, H.; Berg, A.; Chen, Y.J, et al. Systemic delivery of oncolytic adenoviruses targeting transforming growth factor-beta inhibits established bone metastasis in a prostate cancer mouse model. *Hum Gene Ther.* **2012**, *23*, 871–882, https://doi.org/10.1089/hum.2012.040.
41. Javelaud, D.;Alexaki, V.I.; Dennler, S.; Mohammad, K.S.; Guise, T.A.; Mauviel, A. TGFbeta/ SMAD/GLI2 signaling axis in cancer progression and metastasis. *Cancer Res.* **2011**, *71*, 5606–5610, https://doi.org/10.1158/0008-5472.CAN-11-1194.
42. Mohammad, K.S.; Javelaud, D.; Fournier, P.G.; Niewolna, M.; McKenna, C.R.; Peng, X.H, et al. TGF-beta-RI kinase inhibitor SD-208 reduces the development and progression of melanoma bone metastases. *Cancer Res.* **2011**, *71*, 175–184, https://doi.org/10.1158/0008-5472.CAN-10-2651.
43. Juarez, P.; Guise, T.A. TGF-beta in cancer and bone: implications for treatment of bone metastases. Bone. **2011**, *48*, 23–29, https://doi.org/10.1016/j.bone.2010.08.004.
44. Clezardin, P.; Ebetino, F.H.; Fournier, P.G.; Bisphosphonates and cancer-induced bone disease: beyond their antiresorptive activity. *Cancer Res.* **2005**, *65*, 4971–4974, https://doi.org/10.1158/0008-5472.CAN-05-0264.

45. Russell, R.G.; Smith , R.; Preston, C.; Walton, R.J.; Woods, C.G. Diphosphonates in Paget's disease. *Lancet* **1974**, *1*, 894–898, https://doi.org/10.1016/s0140-6736(74)90347-x.
46. Ebetino, F.H.; Hogan, A.M.; Sun, S.; Tsoumpra, M.K.; Duan, X.; Triffitt, J.T.; Kwaasi, A.A.; Dunford, J.E.; Barnett, B.L.; Oppermann, U.; Lundy, M.W.; Boyde, A.; Kashemirov, B.A.; McKenna, C.E.; Russell, R.G.The relationship between the chemistry and biological activity of the bisphosphonates. *Bone.* **2011**, *49*, 20-33, https://doi.org/10.1016/j.bone.2011.03.774.
47. Fleisch, H.; Russell, R.G.; Francis, M.D. Diphosphonates inhibit hydroxyapatite dissolution in vitro and bone resorption in tissue culture and in vivo. *Science*. **1969**, *165*, 1262–1264, https://doi.org/10.1126/science.165.3899.1262.
48. Padalecki, S.S.; Guise, T.A. Actions of bisphosphonates in animal models of breast cancer. Breast Cancer Research **2002**, *4*, 35–41, https://doi.org/10.1186/bcr415.
49. Epstein, S.; Zaidi, M. Biological properties and mechanism of action of ibandronate: application to the treatment of osteoporosis. *Bone.* **2005**, *37*, 433–440, https://doi.org/10.1016/j.bone.2005.05.007.
50. Fromigue' O.; Lagneaux, L.; Body, J.J. Bisphosphonates induce breast cancer cell death in vitro. Journal of Bone and Mineral Research, **2000**, *15*, 2211–2221, https://doi.org/10.1359/jbmr.2000.15.11.2211.
51. Bauss, F.; Body, J.J. Ibandronate in metastatic bone disease: a review of preclinical data. *Anticancer Drugs.* **2005**, *16*, 107–118, https://doi.org/10.1097/00001813-200502000-00001.
52. Sato, M.; Grasser, W.; Endo, N.; Akins, R.; Simmons, H.; Thompson, D.D, et al. Bisphosphonate action. Alendronate localization in rat bone and effects on osteoclast ultrastructure. *J Clin Invest*. **1991**, *88*, 2095–2105, https://doi.org/10.1172/JCI115539.
53. Gainford, M.C.; Dranitsaris, G.; Clemons, M. Recent developments in bisphosphonates for patients with metastatic breast cancer. *BMJ*. **2005**, *330*, 769, https://doi.org/10.1136/bmj.330.7494.769.
54. Kamm, L.; McIlwraith, W.; Kawcak, C . A review of the Efficacy of Tiludronate in the Horse *Journal of Equine Veterinary Science*. **2008**, *28*, 209–214, https://doi.org/10.1016/j.jevs.2008.02.007.
55. Fischer, Jnos.; Ganellin, C.; Robin .*Analogue-based Drug Discovery*. John Wiley & Sons. **2006**, p. 523.
56. Wardley, A.; Davidson, N.; Barrett-Lee, P.; Hong, A.; Mansi, J.; Dodwell, D.; et al. Zoledronic acid significantly improves pain scores and quality of life in breast cancer patients with bone metastases: a randomised, crossover study of community vs hospital bisphosphonate administration. *Br. J. Cancer* **2005**, *92*, 1869–1876, https://doi.org/10.1038/sj.bjc.6602551.
57. Bucay, N.; Osteogenic regulation of vascular calcification: An early perspective**,** *AJP Endocrinology and Metabolism* , **2004**, 286(5):E686-96, DOI:10.1152/ajpendo.00552.2003
58. Lacey, D.L.; Tan, H.L.; Lu, J.; Kaufman, S.; Van, G.; Qiu, W.; et al. Osteoprotegerin ligand modulates murine osteoclast survival in vitro and in vivo. *Am J Pathol.* **2000**, *157*, 435–448, https://doi.org/10.1016/S0002-9440(10)64556-7.
59. Body, J.J.; Greipp, P.; Coleman, R.E.; Facon, T.; Geurs, F.; Fermand , J.P, et al. A phase I study of AMGN-0007, a recombinant osteoprotegerin construct, in patients with multiple myeloma or breast carcinoma related bone metastases. *Cancer* **2003**, *97*, 887–892, https://doi.org/10.1002/cncr.11138.
60. Body, J.J.; Facon, T.; Coleman, R.E.; Lipton, A.; Geurs, F.; Fan, M.; et al. A study of the biological receptor activator of nuclear factor-kappaB ligand inhibitor, denosumab, in patients with multiple myeloma or bone metastases from breast cancer. *Clin Cancer Res.* **2006**, *12*, 1221–1228, https://doi.org/10.1158/1078-0432.CCR-05-1933.
61. Smith, M.R.; Saad, F.; Coleman, R.; Shore, N.; Fizazi, K.; Tombal, B.; et al. Denosumab and bone-metastasis-free survival in men with castration-resistant prostate cancer: results of a phase 3, randomised, placebo-controlled trial. *Lancet*, **2012**, *379*, 39–46, https://doi.org/10.1016/S0140-6736(11)61226-9.
62. Russell, RG .; Bisphosphonates: The first 40 years. Bone **2011**, *49*, 2–19, https://doi.org/10.1016/j.bone.2011.04.022.
63. Wilson, C.; Holen, I.; Coleman, R.E . Seed, soil and secreted hormones: potential interactions of breast cancer cells with their endocrine/paracrine microenvironment and implications for treatment with bisphosphonates. *Cancer Treat Rev*. **2012**, *38*, 877–889, https://doi.org/10.1016/j.ctrv.2012.02.007.
64. Coleman, R.; Gnant, M.; Morgan, G.; Clezardin, P. Effects of bone-targeted agents on cancer progression and mortality. *J Natl Cancer Inst*. **2012**, *104*, 1059–1067, https://doi.org/10.1093/jnci/djs263.
65. Gnant, M.; et al. Endocrine therapy plus zoledronic acid in premenopausal breast cancer. *N Engl J Med*, **2009**, *360*, 679–691, https://doi.org/10.1056/NEJMoa0806285.
66. Coleman, R.E.; et al. Breast-cancer adjuvant therapy with zoledronic acid. *N Engl J Med*, **2011**, *365*, 1396–1405, https://doi.org/10.1056/NEJMoa1105195.

67. Coleman, R.; et al. Zoledronic acid (zoledronate) for postmenopausal women with early breast cancer receiving adjuvant letrozole (ZO-FAST study): Final 60-month results. *Ann Oncol* **2011**, *24*, 398–405, https://doi.org/10.1093/annonc/mds277.
68. Rennert, G.; Pinchev, M.; Rennert , H.S.; Gruber, S.B . Use of bisphosphonates and reduced risk of colorectal cancer. *J Clin Oncol* **2011**, *29*, 1146–1150, https://doi.org/10.1200/JCO.2010.33.7485.
69. Sendur, M.A.; et al. Demographic and clinico-pathological characteristics of breast cancer patients with history of oral alendronate use. *Med Oncol* **2012**, *29*, 2601–2605, https://doi.org/10.1007/s12032-012-0209-9.
70. Clézardin, P.; Massaia, M. Nitrogen-containing bisphosphonates and cancer immunotherapy. *Curr Pharm Des* **2010**, *16*, 3007–3014, https://doi.org/10.2174/138161210793563545.
71. Maniar, A.; et al. Human gammadelta T lymphocytes induce robust NK cellmediated antitumor cytotoxicity through CD137 engagement. *Blood*, **2010**, *116*, 1726–1733, https://doi.org/10.1182/blood-2009-07-234211.
72. Benzaïd, I.; et al. High phosphoantigen levels in bisphosphonate-treated human breast tumors promote Vgamma9Vdelta2 T-cell chemotaxis and cytotoxicity in vivo. *Cancer Res* **2011**, *71*, 4562–4572, https://doi.org/10.1158/0008-5472.CAN-10-3862.
73. Inoue, R.; et al. The inhibitory effect of alendronate, a nitrogen-containing bisphosphonate on the PI3K-Akt-NFkappaB pathway in osteosarcoma cells. *Br J Pharmacol* **2005**, *146*, 633–641, https://doi.org/10.1038/sj.bjp.0706373.
74. Di Salvatore ,M.; et al. Anti-tumour and anti-angiogenetic effects of zoledronic acid on human non-small-cell lung cancer cell line. Cell Prolif **2011**, *44*, 139–146, https://doi.org/10.1111/j.1365-2184.2011.00745.x.
75. Tang, X.; et al. Bisphosphonates suppress insulin-like growth factor 1-induced angiogenesis via the HIF-1alpha/VEGF signaling pathways in human breast cancer cells. *Int J Cancer* **2010**, *126*, 90–103, https://doi.org/10.1002/ijc.24710.
76. Stresing V, et al. Nitrogen-containing bisphosphonates can inhibit angiogenesis in vivo without the involvement of farnesyl pyrophosphate synthase. *Bone*. **2011**, *48*, 259–266, https://doi.org/10.1016/j.bone.2010.09.035.
77. Ding , L.; et al. Somatic mutations affect key pathways in lung adenocarcinoma. *Nature* **2008**, *455* ,1069–1075, https://doi.org/10.1038/nature07423.
78. Ciardiello, F.; Tortora , G .; EGFR antagonists in cancer treatment. *N Engl J Med*, **2008**, *358*, 1160–1174, https://doi.org/10.1056/NEJMra0707704.
79. Yuen, T.; Stachnika, A.; Iqbala, J.; Sgobbab, M.; Guptaa, Y et al. Bisphosphonates inactivate human EGFRs to exert antitumor actions, *Proc Natl Acad Sci U S A*. **2014**, 111, 17989–17994, https://doi.org/10.1073/pnas.1421410111.
80. Rosen, C.J.; Tenenhouse, A .Biochemical markers of bone turnover- A look at laboratory tests that reflect bone status. Postgrad Med. **1998**, *104*, 101-118, https://doi.org/10.3810/pgm.1998.10.447.
81. Delmas, P.D.; Eastell, R.;Garnero, P.;Seibel,.M.J.; Stephen, J.; The use of biochemical Markers of Bone Turnover in Osteoporosis. *Osteoporos Int*. **2000**, *11*, 2-17, https://doi.org/10.1007/s001980070002.
82. Dresner-Pollak, R.; Parker, R.A.; Piku, M.; Thompson, J.; Seibel, M.J.; Greenspan, S.L. Biochemical markers of bone turnover reflect femoral bone loss in elderly women. *Calcif Tissue Int*. **1996**, *59*, 328-33, https://doi.org/10.1007/s002239900135.
83. Delmas, P.D.What do we know about biochemical bone markers? *Bailliers Clin obstet gynaecol*. **1991**, *5*, 817-30, https://doi.org/10.1016/s0950-3552(05)80289-5.
84. Sinigaglia, L.; Varenna, M.; Binnelli, L.; et al. Serum levels of pyridinium crosslinks in postmenopausal women and in pagets disease of bone. *Calcif Tissue Int* .**1997**, *61*, 279-284, https://doi.org/10.1007/s002239900336.
85. Yang, J.M.; Chen C.C. GEMDOCK: A generic evolutionary method for molecular docking, *Proteins*. **2004**, *55*, 288-304, https://doi.org/10.1002/prot.20035.
86. Yang, J.M. Development and evaluation of a generic evolutionary method for protein-ligand docking, J Comput Chem. **2004**. *25*, 843-857, https://doi.org/10.1002/jcc.20013.
87. Yang J.M.; Shen, T.M. A pharmacophore-based evolutionary approach for screening selective estrogen receptor modulators, *Proteins.* **2005**, *59*, 205-220, https://doi.org/10.1002/prot.20387.
88. Heinz, H.; Lin , T-J.; Kishore Mishra, R.; Emami, F.S.; Thermodynamically Consistent Force Fields for the Assembly of Inorganic, Organic, and Biological Nanostructures: The INTERFACE Force Field. *Langmui*r**.** **2013**, *29*, 1754-65, https://doi.org/10.1021/la3038846.

89. Lin, T-J.; Heinz, H. Accurate Force Field Parameters and pH Resolved Surface Models for Hydroxyapatite to Understand Structure, Mechanics, Hydration, and Biological Interfaces. *J. Phys. Chem. C.* **2016**, *120*, 4975-92, https://doi.org/10.1021/acs.jpcc.5b12504.
90. Monajjemi, M.; Mahdavian, L.; Mollaamin, F.; Khaleghian, M. Interaction of Na, Mg, Al, Si with carbon nanotube (CNT): NMR and IR study. *Russ. J. Inorg. Chem* **2009**, *54*, 1465-1473, https://doi.org/10.1134/S0036023609090216.
91. Ghalandari, B.; Monajjemi, M.; Mollaamin, F. Theoretical Investigation of Carbon Nanotube Binding to DNA in View of Drug Delivery. *J.Comput.Theor.Nanosci* **2011**, *8*, 1212-1219, https://doi.org/10.1166/jctn.2011.1801.
92. Khaleghian, M.; Zahmatkesh, M.; Mollaamin, F.; Monajjemi, M. Investigation of Solvent Effects on Armchair Single-Walled Carbon Nanotubes: A QM/MD Study. *Fuller. Nanotub. Carbon Nanostructures.* **2011,** *19*, 251-261, https://doi.org/10.1080/15363831003721757.
93. Bakhshi, K.; Mollaamin, F.; Monajjemi, M. Exchange and correlation effect of hydrogen chemisorption on nano V(100) surface: A DFT study by generalized gradient approximation (GGA). *J.Comput.Theor.Nanosci* **2011**, *8*,763-768, https://doi.org/10.1166/jctn.2011.1750.
94. Tahan, A.; Mollaamin, F.; Monajjemi, M. Thermochemistry and NBO analysis of peptide bond: Investigation of basis sets and binding energy. *Russ. J. Phys. Chem. A* **2009**, *83*, 587-597, https://doi.org/10.1134/S003602440904013X.
95. Mollaamin, F.; Monajjemi, M. Harmonic Linear Combination and Normal Mode Analysis of Semiconductor Nanotubes Vibrations. *J. Comput. Theor. Nanosci* **2015**, *12*, 1030-1039, https://doi.org/10.1166/jctn.2015.3846.
96. Monajjemi, M. Cell membrane causes the lipid bilayers to behave as variable capacitors: A resonance with self-induction of helical proteins. *Biophysical Chemistry* **2015**, *207*, 114-127, https://doi.org/10.1016/j.bpc.2015.10.003.
97. Monajjemi, M. Liquid-phase exfoliation (LPE) of graphite towards graphene: An ab initio study. *Journal of Molecular Liquids* **2017**, *230*, 461–472, https://doi.org/10.1016/j.molliq.2017.01.044.
98. Mahdavian, L.; Monajjemi, M. Alcohol sensors based on SWNT as chemical sensors: Monte Carlo and Langevin dynamics simulation. *Microelectronics journal* **2010**, *41*, 142-149, https://doi.org/10.1016/j.mejo.2010.01.011.
99. Monajjemi, M.; Bagheri, S.; Moosavi, M.S. *et al.* Symmetry breaking of B2N(-,0,+): An aspect of the electric potential and atomic charges. *Molecules* **2015**, *20*, 21636-21657, https://doi.org/10.3390/molecules201219769.
100. Monajjemi, M.; Mohammadian, N.T. S-NICS: An aromaticity criterion for nano molecules. *Journal of Computational and Theoretical Nanoscience* **2015**, *12*, 4895-4914, https://doi.org/10.1166/jctn.2015.4458.
101. Mollaamin, F.; Monajjemi, M.; Salemi, S.; Baei, M.T. A Dielectric Effect on Normal Mode Analysis and Symmetry of BNNT Nanotube. *Fuller. Nanotub. Carbon Nanostructures* **2011**, *19*, 182-196, https://doi.org/10.1080/15363831003782932.
102. Monajjemi, M.; Lee, V.S.; Khaleghian, M.; Honarparvar, B.; Mollaamin, F. Theoretical Description of Electromagnetic Nonbonded Interactions of Radical, Cationic, and Anionic NH2BHNBHNH2 Inside of the B18N18 Nanoring. *J. Phys. Chem C* **2010**, *114*, 15315-15330, https://doi.org/10.1021/jp104274z.
103. Monajjemi, M.; Boggs, J.E. A New Generation of BnNn Rings as a Supplement to Boron Nitride Tubes and Cages. *J. Phys. Chem. A* **2013**, *117*, 1670-1684, http://dx.doi.org/10.1021/jp312073q.
104. Monajjemi, M. Non bonded interaction between BnNn (stator) and BN B (rotor) systems: A quantum rotation in IR region. *Chemical Physics* **2013**, *425*, 29-45, https://doi.org/10.1016/j.chemphys.2013.07.014.
105. Monajjemi, M.; Robert, W.J.; Boggs, J.E. NMR contour maps as a new parameter of carboxyl's OH groups in amino acids recognition: A reason of tRNA–amino acid conjugation. *Chemical Physics* **2014**, *433*, 1-11, https://doi.org/10.1016/j.chemphys.2014.01.017.
106. Monajjemi, M. Quantum investigation of non-bonded interaction between the B15N15 ring and BH2NBH2 (radical, cation, and anion) systems: a nano molecularmotor. *Struct Chem* **2012,** *23*, 551–580, http://dx.doi.org/10.1007/s11224-011-9895-8.
107. Monajjemi, M. Metal-doped graphene layers composed with boron nitride–graphene as an insulator: a nanocapacitor. *Journal of Molecular Modeling* **2014**, *20*, 2507, https://doi.org/10.1007/s00894-014-2507-y.
108. Monajjemi, M.; Heshmat, M.; Haeri, H.H.; Kaveh, F. Theoretical study of vitamin properties from combined QM-MM methods: Comparison of chemical shifts and energy. *Russian Journal of Physical Chemistry* **2006**, *80*, 1061, https://doi.org/10.1134/S0036024406070119.

109. Monajjemi, M.; Honaparvar, B.; Khalili Hadad, B.; Ilkhani, A.; Mollaamin, F. Thermo-Chemical Investigation and NBO Analysis of Some anxileotic as Nano- Drugs. *African journal of pharmacy and pharmacology* **2010**, *4*, 521-529, https://doi.org/10.5897/AJPP.9000278.
110. Monajjemi, M.; Najafpour, J.; Mollaamin, F. $(3,3)_4$ Armchair carbon nanotube in connection with PNP and NPN junctions: Ab Initio and DFT-based studies. *Fullerenes Nanotubes and Carbon Nanostructures* **2013**, *21*, 213-232, https://doi.org/10.1080/1536383X.2011.597010.
111. Monajjemi, M.; Jafari Azan, M.; Mollaamin, F. Density functional theory study on B30N20 nanocage in structural properties and thermochemical outlook. *Fullerenes Nanotubes and Carbon Nanostructures* **2013**, *21*, 503-515, https://doi.org/10.1080/1536383X.2011.629762.
112. Monajjemi, M.; Baie, M.T.; Mollaamin, F. Interaction between threonine and cadmium cation in [Cd(Thr)] (n = 1-3) complexes: Density functional calculations , *Russian Chemical Bulletin*, **2010**, *59*, 886-889, https://doi.org/10.1007/s11172-010-0181-5.
113. Monajjemi, M.; Baheri, H.; Mollaamin, F. A percolation model for carbon nanotube-polymer composites using the Mandelbrot-Given. *Journal of Structural Chemistry* **2011**, *52*, 54-59, https://doi.org/10.1134/S0022476611010070.
114. Sarasia, E.M.; Afsharnezhad, S.; Honarparvar, B.; Mollaamin, F.; Monajjemi, M. Theoretical study of solvent effect on NMR shielding tensors of luciferin derivatives. *Phys Chem Liquids* **2011**, *49*, 561-571, https://doi.org/10.1080/00319101003698992.
115. Monajjemi, M.; Mollaamin, F.; Gholami, M.R.; Yoosbashizadeh, H.; Sadrnezhad, S.K.; Passdar, H. Quantum Chemical Parameters of Some Organic Corrosion Inhibitors, Pyridine, 2-Picoline 4-Picoline and 2,4-Lutidine, Adsorption at Aluminum Surface in Hydrochloric and Nitric Acids and Comparison Between Two Acidic Media. *Main Group Met. Chem.* **2003**, *26*, 349-362, https://doi.org/10.1515/MGMC.2003.26.6.349.
116. Goldstein ,J. L.; Brown, M. S. Regulation of the mevalonate pathway. *Nature* **1990**, *343*, 425–430, https://doi.org/10.1038/343425a0.
117. Rogers,M.J. New insights into the molecular mechanisms of action of bisphosphonates. *Curr. Pharm. Des.* **2003**, *9*, 2643–2658, https://doi.org/10.2174/1381612033453640.
118. Dunford, J. E.; Thompson, K.; Coxon, F. P.; Luckman, S. P.; Hahn, F. M.; Poulter, C. D.; Ebetino, F. H.; Rogers M. J. J. Structure-activity relationships for inhibition of farnesyl diphosphate synthase in vitro and inhibition of bone resorption in vivo by nitrogen-containing bisphosphonates. *Pharmacol. Exp. Ther*. **2001**, *296*, 235–242. http://jpet.aspetjournals.org
119. Rodan G. A.; Reszka A.A. Bisphosphonate mechanism of action. *Curr. Mol. Med***. 2002**, *2*, 571–577, https://doi.org/10.2174/1566524023362104.
120. Russell R. G., Rogers M. J. Bisphosphonates: from the laboratory to the clinic and back again. *Bone*. **1999**, *25*, 97–106, https://doi.org/10.1016/s8756-3282(99)00116-7.
121. Brooks, B.R.; Brooks, C.L.; Mackerell Jr.,A.D.; Nilsson, L.; Petrella, R.J.; Roux, B.; Won, Y.; Archontis, G.; Bartels, C.; Boresch, S.; et al. CHARMM: The Biomolecular Simulation Program, *J Comput Chem*. **2009**, *30*, 1545–1614, https://doi.org/10.1002/jcc.21287.
122. Smrke, A.; Anderson, P.M.; Gulia, A.; Gennatas, S.; Huang, P.H.; Jones, R.L. Future Directions in the Treatment of Osteosarcoma. *Cells* **2021**, *10*, 172, https://doi.org/10.3390/cells10010172.
123. Manzari, M.T.; Shamay, Y.; Kiguchi, H.; Rosen, N.; Scaltriti, M.; Heller, D.A. Targeted drug delivery strategies for precision medicines. *Nat. Rev. Mater.* **2021**, *6*, 351–370, https://doi.org/10.1038/s41578-020-00269-6.
124. Maleki Dana, P.; Hallajzadeh, J.; Asemi, Z.; Mansournia, M.A.; Yousefi, B. Chitosan applications in studying and managing osteosarcoma. *Int. J. Biol. Macromol.* **2021**, *169*, 321–329, https://doi.org/10.1016/j.ijbiomac.2020.12.058.
125. Xu, Y.; Zhang, Z.; Wang, H.; Zhong, W.; Sun, C.; Sun, W.; Wu, H. Zoledronic Acid-Loaded Hybrid Hyaluronic Acid/Polyethylene Glycol/Nano-Hydroxyapatite Nanoparticle: Novel Fabrication and Safety Verification. *Front. Bioeng. Biotechnol.* **2021**, *9*, 629928, https://doi.org/10.3389/fbioe.2021.629928.
126. Zhang, Y.; Yuan, T.; Li, Z.; Luo, C.; Wu, Y.; Zhang, J.; Zhang, X.; Fan, W. Hyaluronate-Based Self-Stabilized Nanoparticles for Immunosuppression Reversion and Immunochemotherapy in Osteosarcoma Treatment. *ACS Biomater. Sci. Eng.* **2021**, *7*, 1515–1525, https://doi.org/10.1021/acsbiomaterials.1c00081.
127. Araki, Y.; Yamamoto, N.; Hayashi, K.; Takeuchi, A.; Miwa, S.; Igarashi, K.; Higuchi, T.; Abe, K.; Taniguchi, Y.; Yonezawa, H.; et al. The number of osteoclasts in a biopsy specimen can predict the efficacy of neoadjuvant chemotherapy for primary osteosarcoma. *Sci. Rep.* **2021**, *11*, 1–9, https://doi.org/10.1038/s41598-020-80504-w.

128. Hofbauer, L.C.; Bozec, A.; Rauner, M.; Jakob, F.; Perner, S.; Pantel, K. Novel approaches to target the microenvironment of bone metastasis. *Nat. Rev. Clin. Oncol.* **2021**, *18*, 488-505, https://doi.org/10.1038/s41571-021-00499-9.
129. Ali, A.; Hoyle, A.; Haran, Á.M.; Brawley, C.D.; Cook, A.; Amos, C.; Calvert, J.; Douis, H.; Mason, M.D.; Dearnaley, D.; et al. Association of Bone Metastatic Burden with Survival Benefit from Prostate Radiotherapy in Patients With Newly Diagnosed Metastatic Prostate Cancer: A Secondary Analysis of a Randomized Clinical Trial. *JAMA Oncol.* **2021**, *7*, 555-563, https://doi.org/10.1001/jamaoncol.2020.7857.
130. Younis,M.H.;Fuentes-Rivera,L.;Summers,S.;Pretell-Mazzini,J. Survival in patients with carcinomas presenting with bone metastasis at diagnosis: A SEER population-based cohort study. *Arch. Orthop. Trauma Surg.* **2021**, *141*, 367–373, https://doi.org/10.1007/s00402-020-03417-3.
131. De Andrade, K.C.; Khincha, P.P.; Hatton, J.N.; Frone, M.N.; Wegman-Ostrosky, T.; Mai, P.L.; Best, A.F.; Savage, S.A. Cancer incidence, patterns, and genotype-phenotype associations in individuals with pathogenic or likely pathogenic germline TP53 variants: An observational cohort study. *Lancet Oncol.* **2021**, *22*, 1787–1798, https://doi.org/10.1016/S1470-2045(21)00580-5.
132. Gill, J.; Gorlick, R. Advancing therapy for osteosarcoma. *Nat. Rev. Clin. Oncol.* **2021**, *18*, 609–624, https://doi.org/10.1038/s41571-021-00519-8.
133. Hiraga, H.; Ozaki, T. Adjuvant and neoadjuvant chemotherapy for osteosarcoma: JCOG Bone and Soft Tissue Tumor Study Group. *Jpn. J. Clin. Oncol.* **2021**, *51*, 1493–1497, https://doi.org/10.1093/jjco/hyab120.
134. Lavit, E.; Aldea, M.; Piperno-Neumann, S.; Firmin, N.; Italiano, A.; Isambert, N.; Kurtz, J.E.; Delcambre, C.; Lebrun, V.; SoibinetOudot, P.; et al. treatment of 120 adult osteosarcoma patients with metachronous and synchronous metastases: A retrospective series of the French Sarcoma Group. *Int. J. Cancer* **2022**, *150*, 645–653, https://doi.org/10.1002/ijc.33823.
135. Gaspar, N.; Campbell-Hewson, Q.; Gallego Melcon, S.; Locatelli, F.; Venkatramani, R.; Hecker-Nolting, S.; Gambart, M.; Bautista, F.; Thebaud, E.; Aerts, I.; et al. Phase I/II study of single-agent lenvatinib in children and adolescents with refractory or relapsed solid malignancies and young adults with osteosarcoma (ITCC-050)I. *ESMO Open* **2021**, *6*, 100250, https://doi.org/10.1016/j.esmoop.2021.100250.
136. Gaspar, N.; Venkatramani, R.; Hecker-Nolting, S.; Melcon, S.G.; Locatelli, F.; Bautista, F.; Longhi, A.; Lervat, C.; Entz-Werle, N.; Casanova, M.; et al. Lenvatinib with etoposide plus ifosfamide in patients with refractory or relapsed osteosarcoma (ITCC-050): A multicentre, open-label, multicohort, phase 1/2 study. *Lancet Oncol.* **2021**, *22*, 1312–1321, https://doi.org/10.1016/S1470-2045(21)00387-9.
137. NCCN guideline bone cancer 2022 v2 National Comprehensive Cancer Network. Bone Cancer (ver. 2.2022). Available online: http://www.nccn.org/professionals/physician_gls/pdf/bone.pdf (accessed on 20 December 2021).
138. Yu, A.L.; Gilman, A.L.; Ozkaynak, M.F.; Naranjo, A.; Diccianni, M.B.; Gan, J.; Hank, J.A.; Batova, A.; London, W.B.; Tenney, S.C.; et al. Long-term follow-up of a phase III study of ch14.18 (dinutuximab) + cytokine immunotherapy in children with high-risk neuroblastoma: COG Study ANBL0032. *Clin. Cancer Res.* **2021**, *27*, 2179–2189, https://doi.org/10.1158/1078-0432.CCR-20-3909.
139. Riudavets, M.; Sullivan, I.; Abdayem, P.; Planchard, D. Targeting HER2 in non-small-cell lung cancer (NSCLC): A glimpse of hope? An updated review on therapeutic strategies in NSCLC harbouring HER2 alterations. *ESMO Open* **2021**, *6*, 100260, https://doi.org/10.1016/j.esmoop.2021.100260.
140. Doroshow, D.B.; Bhalla, S.; Beasley, M.B.; Sholl, L.M.; Kerr, K.M.; Gnjatic, S.; Wistuba, I.I.; Rimm, D.L.; Tsao, M.S.; Hirsch, F.R. PD-L1 as a biomarker of response to immune-checkpoint inhibitors. *Nat. Rev. Clin. Oncol.* **2021**, *18*, 345–362, https://doi.org/10.1038/s41571-021-00473-5.
141. Boye, K.; Longhi, A.; Guren, T.; Lorenz, S.; Næss, S.; Pierini, M.; Taksdal, I.; Lobmaier, I.; Cesari, M.; Paioli, A.; et al. Pembrolizumab in advanced osteosarcoma: Results of a single-arm, open-label, phase 2 trial. *Cancer Immunol. Immunother.* **2021**, *70*, 2617–2624, https://doi.org/10.1007/s00262-021-02876-w.
142. Asaftei, S.D.; Puma, N.; Paioli, A.; Petraz, M.; Morosi, C.; Podda, M.; Tamburini, A.; Palmerini, E.; Coccoli, L.; Grignani, G.; et al. Front-line window therapy with temozolomide and irinotecan in patients with primary disseminated multifocal Ewing sarcoma: Results of the ISG/AIEOP EW-2 Study. *Cancers* **2021**, *13*, 3046, https://doi.org/10.3390/cancers13123046.
143. Leavey, P.J.; Laack, N.N.; Krailo, M.D.; Buxton, A.; Randall, R.L.; DuBois, S.G.; Reed, D.R.; Grier, H.E.; Hawkins, D.S.; Pawel, B.; et al. Phase III trial adding vincristine-topotecan-cyclophosphamide to the initial treatment of patients with nonmetastatic Ewing sarcoma: A Children's Oncology Group Report. *J. Clin. Oncol.* **2021**, *39*, 4029–4038, https://doi.org/10.1200/JCO.21.00358.

144. Cranmer, L.D.; Chau, B.; Mantilla, J.G.; Loggers, E.T.; Pollack, S.M.; Kim, T.S.; Kim, E.Y.; Kane, G.M.; Thompson, M.J.; Harwood, J.L.; et al. Is chemotherapy associated with improved overall survival in patients with dedifferentiated chondrosarcoma? A SEER database analysis. *Clin. Orthop. Relat. Res.* **2021**, *14*, 748–758, https://doi.org/10.1097/CORR.0000000000002011.
145. Hompland, I.; Ferrari, S.; Bielack, S.; Palmerini, E.; Hall, K.S.; Picci, P.; Hecker-Nolting, S.; Donati, D.M.; Blattmann, C.; Bjerkehagen, B.; et al. Outcome in dedifferentiated chondrosarcoma for patients treated with multimodal therapy: Results from the EUROpean Bone Over 40 Sarcoma Study. *Eur. J. Cancer* **2021**, *151*, 150–158, https://doi.org/10.1016/j.ejca.2021.04.017.
146. Duffaud, F.; Italiano, A.; Bompas, E.; Rios, M.; Penel, N.; Mir, O.; Piperno-Neumann, S.; Chevreau, C.; Delcambre, C.; Bertucci, F.; et al. Efficacy and safety of regorafenib in patients with metastatic or locally advanced chondrosarcoma: Results of a non-comparative, randomised, double-blind, placebo controlled, multicentre phase II study. *Eur. J. Cancer* **2021**, *150*, 108–118, https://doi.org/10.1016/j.ejca.2021.03.039.
147. Pirozzi, C.J.; Yan, H. The implications of IDH mutations for cancer development and therapy. *Nat. Rev. Clin. Oncol.* **2021**, *18*, 645–661, https://doi.org/10.1038/s41571-021-00521-0.
148. Nagano, A.; Tsugita, M.; Nishimoto, Y.; Akiyama, H.; Kawai, A. The 'other' bone sarcomas in Japan: A retrospective study of primary bone sarcomas other than osteosarcoma, Ewing sarcoma and chondrosarcoma, using data from the Bone Tumuor Registry in Japan. *Jpn. J. Clin. Oncol.* **2021**, *51*, 1430–1436, https://doi.org/10.1093/jjco/hyab090.
149. Stacchiotti, S.; Frezza, A.M.; Blay, J.Y.; Baldini, E.H.; Bonvalot, S.; Bovée, J.V.M.G.; Callegaro, D.; Casali, P.G.; Chiang, R.C.; Demetri, G.D.; et al. Ultra-rare sarcomas: A consensus paper from the Connective Tissue Oncology Society community of experts on the incidence threshold and the list of entities. *Cancer* **2021**, *15*, 2934–2942, https://doi.org/10.1002/cncr.33618.
150. Gusho, C.A.; Weiss, M.C.; Lee, L.; Gitelis, S.; Blank, A.T.; Wang, D.; Batus, M. The clinical utility of next-generation sequencing for bone and soft tissue sarcoma. *Acta Oncol.* **2022**, *61*, 38–44, https://doi.org/10.1080/0284186X.2021.1992009.
151. Zhan, H.; Mo, F.; Zhu, M.; Xu, X.; Zhang, B.; Liu, H.; Dai, M. A SEER-based nomogram accurately predicts prognosis in Ewing's sarcoma. *Sci. Rep.* **2021**, *11*, 22723, https://doi.org/10.1038/s41598-021-02134-0.
152. Zadeh, M.A.A.; Lari, H.; Kharghanian, L.; Balali, E.; Khadivi, R.; Yahyaei, H.; Mollaamin, F.; Monajjemi, M. Density functional theory study and anticancer properties of shyshaq plant: In view point of nano biotechnology. *J. Comput. Theor. Nanosci*.**2015**, *12*, 4358-4367, https://doi.org/10.1166/jctn.2015.4366.
153. Barker, C.I.S.; Groeneweg, G.; Maitland-van der Zee, A.H.; Rieder, M.J.; Hawcutt, D.B.; Hubbard, T.J.; Swen, J.J.; Carleton, B.C. Pharmacogenomic testing in paediatrics: Clinical implementation strategies. *Br. J. Clin. Pharmacol.* **2022**, 88, 4297-4310, https://doi.org/10.1111/bcp.15181.
154. Groenland, S.L.; Verheijen, R.B.; Joerger, M.; Mathijssen, R.H.J.; Sparreboom, A.; Beijnen, J.H.; Beumer, J.H.; Steeghs, N.; Huitema, A.D.R. Precision dosing of targeted therapies is ready for prime time. *Clin. Cancer Res.* **2021**, *27*, 6644–6652, https://doi.org/10.1158/1078-0432.CCR-20-4555.
155. Pestana, R.C.; Beal, J.R.; Parkes, A.; Hamerschlak, N.; Subbiah, V. Impact of tissue-agnostic approvals for patients with sarcoma. *Trends Cancer* **2021**, *8*, 135–144, https://doi.org/10.1016/j.trecan.2021.11.007.